

NUMERICAL COMPUTATION FOR FREE BOUNDARY OF LIGAND AND
SIGNAL TRANSDUCTION ASSOCIATED WITH THE INVADOPODIA
FORMATION

NOOREHAN BINTI YAACOB

A thesis submitted in fulfilment of the
requirements for the award of the degree of
Doctor of Philosophy

Faculty of Science
Universiti Teknologi Malaysia

SEPTEMBER 2022

DEDICATION

Special dedication to my beloved

ayah, Yaacob Mohamed

mak, Kamariah Mahat

along, Mohamad Redzuan Yaacob

angah, Mohd Radzi Yaacob

alang, Yusliana Yaacob

sister in law, Norhafiezza Abd Ghani

niece, Nur Aqilah Sofia

and

nephew, Shafiy Aisar.

Thank you for the endless love, care, and support during my PhD journey.

ACKNOWLEDGEMENT

In the name of Allah, the Most merciful, Most beneficent, Praise upon the Beloved Prophet, His Family, and Companion. There is no power except by the power of Allah and I humbly return my acknowledgment that all knowledge belongs to Allah.

Throughout the writing of this thesis, I have received a great deal of support and assistance from many people. I would like to acknowledge with great gratitude to the Ministry of Higher Education for the scholarship under the MybrainSC scheme and the Fundamental Research Grant Scheme (FRGS/1/2018/STG06/UTM/02/1).

A special thanks and deepest appreciation to Dr. Mohd Ariff Admon, my main supervisor for his guidance throughout the process of completing this thesis from the initial stage, all the way through the end. I have greatly appreciated his knowledge, patience, and willingness to help me. Not to be forgotten, my gratitude to my co-supervisor, Assoc. Prof. Dr. Sharidan Shafie for his valuable advice, guidance, encouragement, and suggestions throughout the course of this study. My appreciation also extends to Prof. Takashi Suzuki (Osaka University, Japan) and Prof. Clair Poignard (University of Bordeaux, France) for their valuable guidance during my short visit to Japan.

My heartiest gratitude goes to my parents and siblings. Without their understanding and encouragement, it would be impossible for me to complete this study. Finally, I could not have completed this thesis without the support of my special friends (Hanis and Suzarina) who always listen to every problem that I faced while conducting this study. Not to forget, my research mates (Kak Zura and Alin), and all my supportive colleagues who provided happy distractions to rest my mind outside of my research. Your kindness and help will be a great memory for me.

ABSTRACT

Cancer cell invasion in the metastasis process contributes to the high death cases among cancer patients. The spread of tumors from one part to another in the body is a result of the existence of finger-like protrusions or known as invadopodia. The formation of invadopodia involves several molecular processes that include the activity of matrix metalloproteinases (MMPs) in degrading the extracellular matrix (ECM), the creation of ligand, stimulation of signal transduction from the binding of ligand with epidermal growth factor receptor, up-regulation of MMPs, and actin polymerization. The purpose of this study is to investigate the emergence of invadopodia on the plasma membrane through the mathematical model of quasi-static and unsteady cases involving ligand-protein and signal transduction processes. The degradation of the ECM by the MMPs is the starting point for the occurrence of invadopodia formation where the density of MMPs is taken as a trigonometric function. The creation of invadopodia is a result of actin polymerization activity that moves the plasma membrane. Hence, the movement is assumed as the membrane velocity and is accounted for as without and with jump velocity approaches where the jump from ligand to signal occurs. The method of level set is emphasized to detect the movement of the free boundary plasma membrane and is considered as a zero level set function. In addition, the location of the plasma membrane leads to the occurrence of regular points (a point that is far from the interface) and neighboring points (a point that is near to the interface). These points are solved using the second-order centered finite difference method and ghost fluid with the linear extrapolation method. The results showed that the mentioned integrated methods effectively describe the movement of the free boundary plasma membrane and this directly points out the formation of protrusions (invadopodia) on the plasma membrane. Furthermore, the size of the protrusions is observed to become longer as time increases. However, the aggressive (longer) protrusion is detected in the quasi-static model, whereas only small protrusions are spotted in the unsteady model. It is also observed that the disconnection of the plasma membrane happened in the quasi-static model and without jump velocity approach compared to the other problems. Nevertheless, in all problems conducted, the density of ligand and signal is the highest on the interface due to the stimulation of signal through the binding between ligand and membrane-associated receptor that is happening here. Besides, the numerical errors are compared for the three sizes of meshes. The simulation results demonstrated that for all profiles of level set, ligand, and signal, the higher size of meshes provides a smaller value of error compared to the lower size of meshes.

ABSTRAK

Pencerobohan sel kanser dalam proses metastasis menyumbang kepada kes kematian yang tinggi di kalangan pesakit kanser. Penyebaran tumor dari satu bahagian ke bahagian yang lain dalam badan adalah hasil daripada kewujudan tonjolan seperti jari atau dikenali sebagai invadopodia. Pembentukan invadopodia melibatkan beberapa proses molekul yang merangkumi aktiviti matriks metalloproteinase (MMPs) dalam merendahkan matriks ekstraselular (ECM), penciptaan ligan, rangsangan transduksi isyarat daripada pengikatan ligan dengan reseptor faktor pertumbuhan epidermis, pengawalan MMP, dan pempolimeran aktin. Tujuan kajian ini adalah untuk menyiasat kemunculan invadopodia pada membran plasma melalui model matematik kes kuasi-statik dan tak mantap yang melibatkan ligan-protein dan proses transduksi isyarat. Degradasi ECM oleh MMP adalah titik permulaan kepada berlakunya pembentukan invadopodia di mana ketumpatan MMP diambil sebagai fungsi trigonometri. Penciptaan invadopodia adalah hasil daripada aktiviti pempolimeran aktin yang menggerakkan membran plasma. Oleh yang demikian, pergerakan diandaikan sebagai halaju membran dan dikira sebagai tanpa dan dengan pendekatan halaju lompatan di mana lompatan berlaku dari ligan ke isyarat. Kaedah set aras ditekankan untuk mengesan pergerakan membran plasma sempadan bebas dan dianggap sebagai fungsi set aras sifar. Tambahan lagi, lokasi membran plasma membawa kepada berlakunya titik biasa (titik yang jauh dari antara muka) dan jiran (titik yang dekat dengan antara muka). Titik ini diselesaikan menggunakan kaedah beza terhingga berpusat tertib kedua dan bendalir jelmaan dengan kaedah ekstrapolasi linear. Keputusan menunjukkan bahawa kaedah bersepadu yang dinyatakan berkesan menggambarkan pergerakan membran plasma sempadan bebas dan ini secara langsung menunjukkan pembentukan tonjolan (invadopodia) pada membran plasma. Tambahan pula, saiz tonjolan diperhatikan menjadi lebih panjang apabila masa meningkat. Walau bagaimanapun, tonjolan yang agresif (lebih panjang) dikesan dalam model kuasi-statik, manakala hanya tonjolan kecil yang dikesan dalam model tidak mantap. Ia juga diperhatikan bahawa pemotongan membran plasma berlaku dalam model kuasi statik dan tanpa pendekatan halaju lompat berbanding masalah lain. Namun begitu, dalam semua masalah yang dijalankan, ketumpatan ligan dan isyarat adalah paling tinggi pada antara muka disebabkan oleh rangsangan isyarat melalui pengikatan antara ligan dan reseptor berkaitan membran yang berlaku di sini. Selain itu, ralat berangka dibandingkan untuk tiga saiz jejaring. Keputusan simulasi menunjukkan bahawa untuk semua profil set aras, ligan dan isyarat, saiz jejaring yang lebih tinggi memberikan nilai ralat yang lebih kecil berbanding saiz jejaring yang lebih rendah.

TABLE OF CONTENTS

	TITLE	PAGE
	DECLARATION	ii
	DEDICATION	iii
	ACKNOWLEDGEMENT	iv
	ABSTRACT	v
	ABSTRAK	vi
	TABLE OF CONTENTS	vii
	LIST OF TABLES	x
	LIST OF FIGURES	xii
	LIST OF ABBREVIATIONS	xx
	LIST OF SYMBOLS	xxii
1	INTRODUCTION	1
	1.1 Introduction	1
	1.2 Background of the Study	1
	1.2.1 Biological Point of View	2
	1.2.2 Mathematical Point of View	4
	1.3 Problem Statements	6
	1.4 Objectives of the Study	8
	1.5 Scope of the Study	8
	1.6 Significance of the Study	11
	1.7 Thesis Organization	12
2	LITERATURE REVIEW	13
	2.1 Introduction	13
	2.2 Cancer Cell Invasion	13
	2.3 Invadopodia Formation	19
	2.4 Signal Transduction from Ligand-EGFR Binding Leads to Actin Polymerization	22
	2.5 Level Set Method	27
	2.6 Mathematical Formulation for the Invadopodia Formation	29
	2.6.1 Fixed Plasma Membrane	30

2.6.2	Free Boundary Plasma Membrane	33
2.7	Research Gap	35
2.8	Conclusion	39
3	MATHEMATICAL PRELIMINARIES	41
3.1	Introduction	41
3.2	Research Design and Procedure	41
3.2.1	Mathematical Formulation	42
3.2.2	Numerical Methods and Algorithm	42
3.3	Mathematical Modeling	44
3.4	Non-dimensionalization	46
3.5	Numerical Computation and Discretization	52
3.6	Algorithm of the Solution	73
3.7	Conclusion	74
4	QUASI-STATIC LIGAND AND SIGNAL TRANSDUCTION DURING THE INVADOPODIA FORMATION	75
4.1	Introduction	75
4.2	Mathematical Formulation of the Problem	75
4.3	Numerical Computation	77
4.3.1	Level Set Method	78
4.3.2	Finite Difference and Ghost Fluid with Linear Extrapolation Methods	78
4.3.3	Solution Procedure	97
4.4	Results and Discussion	99
4.4.1	Case of Without Jump Velocity	100
4.4.2	Case of With Jump Velocity	109
4.5	Numerical Convergence	117
4.6	Conclusion	121
5	UNSTEADY LIGAND AND SIGNAL TRANSDUCTION DURING THE INVADOPODIA FORMATION	123
5.1	Introduction	123
5.2	Mathematical Formulation of the Problem	124
5.3	Numerical Computation	125
5.3.1	Level Set Method	126

5.3.2	Finite Difference and Ghost Fluid with Linear Extrapolation Methods	126
5.3.3	Solution Procedure	143
5.4	Results and Discussion	144
5.4.1	Case of Without Jump Velocity	145
5.4.2	Case of With Jump Velocity	154
5.5	Numerical Convergence	160
5.6	Conclusion	164
6	CONCLUSION	167
6.1	Introduction	167
6.2	Summary of the Thesis	167
6.3	Suggestions and Recommendations for the Future Research	172
	REFERENCES	175
	APPENDICES	189

LIST OF TABLES

TABLE NO.	TITLE	PAGE
2.1	Summaries of the mathematical modeling and numerical simulation work in recent years (c^* , σ , n , f , and c denote ligand, signal, actin, MMPs, and ECM, respectively).	38
4.1	The boundary conditions applied on the signal region.	88
4.2	The boundary conditions applied on the signal region.	97
4.3	The parameter values used in the numerical computation for the quasi-static mathematical model.	100
4.4	The infinity norm behavior against the total size of meshes for the case of without jump velocity (quasi-static model).	119
4.5	The infinity norm behavior against the total size of meshes for the case of with jump velocity (quasi-static model).	120
5.1	The infinity norm behavior against the total size of meshes for the case of without jump velocity (unsteady model).	162
5.2	The infinity norm behavior against the total size of meshes for the case of with jump velocity (unsteady model).	163
6.1	The comparison between the quasi-static and unsteady models.	171
A.1	The summary of the discretized equations for signal region.	189
A.2	The summary of the discretized equations for ligand region.	190

A.3	The summary of the discretized equations for signal region.	191
A.4	The summary of the discretized equations for ligand region.	192

LIST OF FIGURES

FIGURE NO.	TITLE	PAGE
1.1	The invadopodium formation on the plasma membrane of the tumor cell [10].	3
1.2	Research framework.	10
2.1	The illustration of the angiogenesis process [32].	14
2.2	The metastasis process in the cancer cell invasion for the formation of the secondary tumor [38].	15
2.3	The formation and maturation of invadopodium [56].	19
2.4	The type of ligand with their specified receptor [69].	22
2.5	The flow of information during cell signaling.	24
2.6	The actin assembly regulators [78].	25
2.7	The region for actin is disconnected as $t > 0$ and actin diffused to the extracellular region [12].	36
3.1	The type of points that are involved in the computation.	43
3.2	The geometrical setting of the complete domain for two-dimensional invadopodia formation.	44
3.3	The schematic diagram for the process of invadopodia formation in an invasive cancer cell.	45
3.4	The condition of the extrapolation method for signal at point, B in x -axis.	52
3.5	The radius of a circle.	54
3.6	The distance to the interface for the x -axis, θ_x where the interface (purple line) is located (a) on the left of $u_{i,j}^n$ and (b) on the right of $u_{i,j}^n$.	54
3.7	The distance to the interface for the y -axis, θ_y where the interface (purple line) is located (a) on the below of $u_{i,j}^n$ and (b) on the above of $u_{i,j}^n$.	55

3.8	The neighboring point for ligand position.	57
3.9	The neighboring point for signal position.	58
3.10	The point on the interface, I .	59
3.11	The regular points in the intracellular (signal position).	59
3.12	The neighboring points that are located (a) on the right (dark green) and on the left (light green) of the interface, and (b) on the above (dark blue) and on the below (light blue) of the interface.	60
3.13	The neighboring points that are located (a) on the left (dark brown) and on the right (light brown) of the interface, and (b) on the below (dark grey) and on the above (light grey) of the interface.	60
3.14	The point on the interface (a) right point, I_x^+ and (b) left point, I_x^- .	61
3.15	The point on the interface (a) above point, I_y^+ and (b) below point, I_y^- .	62
3.16	The regular points on the x -axis, R_x .	63
3.17	The regular points on the y -axis, R_y .	63
3.18	The technique of discretization for the velocity computation of the neighboring point in the (a) right, N_x^+ and (b) left, N_x^- sides of the interface in the intracellular region.	63
3.19	The technique of discretization for the velocity computation of the neighboring point in the (a) above, N_y^+ and (b) below, N_y^- sides of the interface in the intracellular region.	64
3.20	The technique of discretization for the velocity computation of the neighboring point in the (a) right, N_{Lx}^+ and (b) left, N_{Lx}^- sides of the interface in the extracellular region.	65

3.21	The technique of discretization for the velocity computation of the neighboring point in the (a) above, N_{Ly}^+ and (b) below, N_{Ly}^- sides of the interface in the extracellular region.	65
3.22	The point on the interface (a) right point, I_x^+ and (b) left point, I_x^- .	66
3.23	The point on the interface (a) above point, I_y^+ and (b) below point, I_y^- .	66
3.24	The technique of discretization for the velocity computation of the neighboring point in the (a) right, N_x^+ and (b) left, N_x^- sides of the interface in the intracellular region.	67
3.25	The method to solve for the velocity of the neighboring point in the intracellular region specifically for the (a) above, N_y^+ and (b) below, N_y^- sides of the interface in the intracellular region.	68
3.26	The method to solve for the velocity from the (a) right, N_{Lx}^+ and (b) left, N_{Lx}^- sides of the interface in the extracellular region.	69
3.27	The method to solve for the velocity from the (a) above, N_{Ly}^+ and (b) below, N_{Ly}^- sides of the interface in the extracellular region.	69
3.28	The domain with the position of the boundary.	70
3.29	The method to solve the velocity extension for the right, $(v_x)^+$ and left, $(v_x)^-$ sides of the interface.	71
3.30	The method to solve the velocity extension for the above, $(v_y)^+$ and below, $(v_y)^-$ sides of the interface.	72
4.1	The regular (A and D) and neighboring (B and C) points.	78
4.2	The interface positions (purple line) are located in between (a) horizontal, (b) vertical, and (c) diagonal neighboring meshes.	79

4.3	Interface located in between two horizontal meshes with left θ_x to the neighboring point.	80
4.4	Interface located in between two horizontal meshes with right θ_x to the neighboring point.	81
4.5	Interface located in between two vertical meshes with below θ_y to the neighboring point.	82
4.6	Interface located in between two vertical meshes with above θ_y to the neighboring point.	83
4.7	Interface located in between four meshes with left θ_x and below θ_y to the neighboring point.	84
4.8	Interface located in between four meshes with left θ_x and above θ_y to the neighboring point.	85
4.9	Interface located in between four meshes with right θ_x and below θ_y to the neighboring point.	86
4.10	Interface located in between four meshes with right θ_x and above θ_y to the neighboring point.	87
4.11	Interface located in between two horizontal meshes with left θ_{Lx} to the neighboring point.	88
4.12	Interface located in between two horizontal meshes with right θ_{Lx} to the neighboring point.	89
4.13	Interface located in between two vertical meshes with below θ_{Ly} to the neighboring point.	90
4.14	Interface located in between two vertical meshes with above θ_{Ly} to the neighboring point.	91
4.15	Interface located in between four meshes with left θ_{Lx} and below θ_{Ly} to the neighboring point.	93
4.16	Interface located in between four meshes with left θ_{Lx} and above θ_{Ly} to the neighboring point.	94
4.17	Interface located in between four meshes with right θ_{Lx} and below θ_{Ly} to the neighboring point.	95
4.18	Interface located in between four meshes with right θ_{Lx} and above θ_{Ly} to the neighboring point.	96

4.19	The flow diagram for the computation of ligand density in quasi-static model.	98
4.20	The flow diagram for the computation of signal density in quasi-static model.	98
4.21	The setting in the numerical computation.	99
4.22	Initial values of the (a) interface position, (b) ligand density, and (c) signal density.	101
4.23	The results for (a) interface position, (b) ligand density, and (c) signal density after 6 time iterations.	102
4.24	The results for (a) interface position, (b) ligand density, and (c) signal density after 8 time iterations.	103
4.25	The results for (a) interface position, (b) ligand density, and (c) signal density after 10 time iterations.	104
4.26	The results for (a) interface position, (b) ligand density, and (c) signal density after 12 time iterations.	105
4.27	The results for (a) interface position, (b) ligand density, and (c) signal density after 14 time iterations.	106
4.28	The results for (a) interface position, (b) ligand density, and (c) signal density after 18 time iterations.	107
4.29	The results for (a) interface position, (b) ligand density, and (c) signal density after 19 time iterations.	108
4.30	The disconnection of plasma membrane after 20 time iterations.	109
4.31	Initial values of the (a) interface position, (b) ligand density, and (c) signal density.	110
4.32	The results for (a) interface position, (b) ligand density, and (c) signal density after 30 time iterations.	111
4.33	The results for (a) interface position, (b) ligand density, and (c) signal density after 50 time iterations.	112
4.34	The results for (a) interface position, (b) ligand density, and (c) signal density after 55 time iterations.	113

4.35	The results for (a) interface position, (b) ligand density, and (c) signal density after 85 time iterations.	114
4.36	The results for (a) interface position, (b) ligand density, and (c) signal density after 95 time iterations.	115
4.37	The results for (a) interface position, (b) ligand density, and (c) signal density after 135 time iterations.	116
4.38	The initial interface at three different sizes of meshes of (a) $M = 50$, (b) $M = 80$, and (c) $M = 100$.	118
4.39	The initial profile of ligand at three different sizes of meshes of (a) $M = 50$, (b) $M = 80$, and (c) $M = 100$.	118
4.40	The initial profile of signal at three different sizes of meshes of (a) $M = 50$, (b) $M = 80$, and (c) $M = 100$.	118
4.41	The convergence profiles for level set, ligand, and signal transduction for quasi-static without jump velocity.	119
4.42	The convergence profiles for level set, ligand, and signal transduction for quasi-static with jump velocity.	120
5.1	The flow diagram for the computation of ligand density in the unsteady model.	143
5.2	The flow diagram for the computation of signal density in the unsteady model.	144
5.3	The initial set up for the (a) interface, (b) ligand density, and (c) signal density.	145
5.4	The accumulation of ligand in the extracellular region for six different computation times (a) $t = 0.01$, (b) $t = 0.02$, (c) $t = 0.03$, (d) $t = 0.04$, (e) $t = 0.05$, and (f) $t = 0.14$.	146
5.5	The diffusion of signal in the intracellular region for six different computation times (a) $t = 0.01$, (b) $t = 0.02$, (c) $t = 0.03$, (d) $t = 0.04$, (e) $t = 0.05$, and (f) $t = 0.14$.	147
5.6	The results for (a) interface position, (b) ligand density, and (c) signal density at $t = 1.1$.	149

5.7	The results for (a) interface position, (b) ligand density, and (c) signal density at $t = 1.5$.	150
5.8	The results for (a) level set, (b) ligand, and (c) signal transduction at $t = 2.0$.	151
5.9	The results for (a) interface position, (b) ligand density, and (c) signal density at $t = 2.5$.	152
5.10	The results for (a) interface position, (b) ligand density, and (c) signal density at $t = 2.8$.	153
5.11	The results for (a) interface position, (b) ligand density, and (c) signal density at $t = 1.1$.	155
5.12	The results for (a) interface position, (b) ligand density, and (c) signal density at $t = 2.3$.	156
5.13	The results for (a) interface position, (b) ligand density, and (c) signal density at $t = 3.1$.	157
5.14	The results for (a) interface position, (b) ligand density, and (c) signal density at $t = 3.9$.	158
5.15	The results for (a) interface position, (b) ligand density, and (c) signal density at $t = 4.4$.	159
5.16	The initial interface at three different sizes of meshes of (a) $M = 50$, (b) $M = 80$, and (c) $M = 100$.	160
5.17	The initial profile of ligand at three different sizes of meshes of (a) $M = 50$, (b) $M = 80$, and (c) $M = 100$.	160
5.18	The initial profile of signal at three different sizes of meshes of (a) $M = 50$, (b) $M = 80$, and (c) $M = 100$.	161
5.19	The convergence profiles for level set, ligand, and signal transduction for the unsteady without jump velocity model.	162
5.20	The convergence profiles for level set, ligand, and signal transduction for the unsteady with jump velocity model.	163
B.1	The extracellular point located on the left of the interface.	194
B.2	The extracellular point located on the right of the interface.	195

B.3	The extracellular point located on the below of the interface.	197
B.4	The extracellular point located on the above of the interface.	198
B.5	The extracellular point located on the left and below of the interface.	200
B.6	The extracellular point located on the left and above of the interface.	201
B.7	The extracellular point located on the right and below of the interface.	202
B.8	The extracellular point located on the right and above of the interface.	203
B.9	The regular point located on the extracellular region.	204

LIST OF ABBREVIATIONS

Abl	-	Abelson Tyrosine-Protein Kinase
AREG	-	Amphiregulin
Arg	-	Abelson-related Gene
Arp2/3	-	Actin Related Protein 2/3
BTC	-	Betacellulin
CRC	-	Colorectal Cancer
DCIS	-	Ductal Carcinoma In Situ
ECM	-	Extracellular Matrix
EGF	-	Epidermal Growth Factor
EGFR	-	Epidermal Growth Factor Receptor
EMT	-	Epithelial-mesenchymal Transition
EPR	-	Epiregulin
FMNL2	-	Formin-like 2
HB-EGF	-	Heparin-Binding EGF-like Growth Factor
IDC	-	Invasive Ductal Carcinoma
LOX	-	Lysyl Oxidase
MDEs	-	Matrix Degrading Enzymes
MMPs	-	Matrix Metalloproteinases
MT1-MMPs	-	Membrane Type-1 Metalloproteinases
Nck1	-	Non-catalytic Region of Tyrosine Kinase Adaptor Protein 1
N-WASP	-	Neuronal WiskottAldrich Syndrome Protein
PAI-1	-	Plasminogen Activator Inhibitor Type-1
PDEs	-	Partial Differential Equations
TGF- α	-	Transforming Growth Factor- α
TGF- β	-	Transforming Growth Factor- β

uPAs	-	Urokinase Plasminogens
uPAR	-	Urokinase Receptor
VEGF	-	Vascular Endothelial Growth Factor
VN	-	Vitronectin
WIP	-	WASp-interacting protein

LIST OF SYMBOLS

c	-	Extracellular matrix
c^*	-	Ligand
c_{Γ}^*	-	Ligand on the interface
$(c^*)_0$	-	Density of ligand at the chemical equilibrium
d_{c^*}	-	Ligand diffusivity rate
d_{σ}	-	Signal diffusivity rate
f	-	Matrix metalloproteinases (MMPs)
g	-	Density of the MMPs
h	-	Step length for x and y -axes
I	-	The point that is located on the interface
I_x^+	-	The point that is located on the interface (right side)
I_x^-	-	The point that is located on the interface (left side)
I_y^+	-	The point that is located on the interface (above side)
I_y^-	-	The point that is located on the interface (below side)
k	-	Time step
L	-	Size of domain
ℓ	-	Characteristic length
M	-	Size of mesh
N	-	Neighboring point
N_x^+	-	Neighboring point in the intracellular region that is located on the right of the interface
N_x^-	-	Neighboring point in the intracellular region that is located on the left of the interface
N_y^+	-	Neighboring point in the intracellular region that is located on the above of the interface
N_y^-	-	Neighboring point in the intracellular region that is located on the below of the interface

N_{Lx}^+	-	Neighboring point in the extracellular region that is located on the right of the interface
N_{Lx}^-	-	Neighboring point in the extracellular region that is located on the left of the interface
N_{Ly}^+	-	Neighboring point in the extracellular region that is located on the above of the interface
N_{Ly}^-	-	Neighboring point in the extracellular region that is located on the below of the interface
n	-	Actin
R_x	-	Regular point on the x -axis
R_y	-	Regular point on the y -axis
r	-	Radius of a circle
\mathbf{v}	-	Velocity of the plasma membrane
\mathbf{v}_1	-	Without jump velocity
\mathbf{v}_2	-	With jump velocity
v_x	-	Velocity for the x -axis in the intracellular region
$(v_x)^+$	-	Velocity from the right side
$(v_x)^-$	-	Velocity from the left side
v_{Lx}	-	Velocity for the x -axis in the extracellular region
v_y	-	Velocity from the y -axis in the intracellular region
$(v_y)^+$	-	Velocity from the above side
$(v_y)^-$	-	Velocity from the below side
v_{Ly}	-	Velocity from the y -axis in the extracellular region
\mathbf{w}	-	Velocity extension

Greek Symbols

Γ	-	Interface
Ω	-	Square domain
$\partial\Omega$	-	Boundary of the square domain
$\partial\Omega_x^+$	-	Right boundary of domain, Ω
$\partial\Omega_x^-$	-	Left boundary of domain, Ω

$\partial\Omega_y^+$	-	Above boundary of domain, Ω
$\partial\Omega_y^-$	-	Below boundary of domain, Ω
ψ	-	Level set function
$(\psi)_0$	-	Characteristic level set function
σ	-	Signal
σ_Γ	-	Signal on the interface
$(\sigma)_0$	-	Density of signal at the chemical equilibrium
τ	-	Characteristic time
θ_x	-	Distance from the point x_i to the interface in the intracellular region
θ_y	-	Distance from the point y_j to the interface in the intracellular region
θ_{Lx}	-	Distance from the point x_i to the interface in the extracellular region
θ_{Ly}	-	Distance from the point y_j to the interface in the extracellular region
$0_t^{c^*}$	-	Extracellular region
0_t^σ	-	Intracellular region

CHAPTER 1

INTRODUCTION

1.1 Introduction

In this chapter, the main area of this study is presented concisely. The background of the study is explained in Section 1.2 where this section is divided into two sub-sections: (1.2.1) biological point of view, and (1.2.2) mathematical point of view. The problem statements corresponding to the aim of this study are explained in Section 1.3. Next, the objectives of solving the proposed problem are stated in Section 1.4. Further, the scope of the study is discussed in Section 1.5. In addition, the significance of the study is explained in Section 1.6. Finally, the thesis organization is clarified in Section 1.7.

1.2 Background of the Study

According to World Health Organization, in the next two decades, the total of death related to cancer will rise by 70% [1]. Cancer is the second-highest cause of death and one out of six deaths that happened globally is due to cancer. The types of cancer that usually occur in men are lung, prostate, colorectal, stomach, and liver while among women are breast, colorectal, lung, cervix, and thyroid cancer [2]. Over the years, the case of cancer is increased. By 2014, it is reported that, in the United States alone, about 1,665,540 people experienced cancer, and 585,720 of them died [2]. Hence, from this large value, cancer is one of the serious problems that can affect human health [3]. Referring to Malaysia, the statistics of cancer patients released by

the national cancer institute showed an increasing trend from 2014 to 2019 and a slight decrease in 2020 [4].

However, the data of cancer patients for 2021 and 2022 is not yet released by the national cancer institute. The decrease of patients in 2020 is because of the establishment and upgrading of treatment facilities such as surgery, radiotherapy, chemotherapy, hormonal therapy, immune therapy, and symptomatic and supportive therapy. In Malaysia, there are 14 radiotherapy centers where patients can seek treatment. In addition, the increase in training of skilled staff in the treatment of cancer also leads to a reduction in the number of cancer patients [5].

Thus, in this section, the occurrence of cancer is explained from the biological and mathematical points of view. In the biological part, the cancer cell invasion is discussed through the explanation at the sub-cellular level where the formation of invadopodia occurs. Meanwhile, from the mathematical view, the invadopodia formation is explained in terms of mathematical modeling.

1.2.1 Biological Point of View

The occurrence of the tumor begins as the genomes of the individual cells in an organism becomes destabilized. In normal conditions, the proto-oncogenes are responsible for cell division and growth but during genetic mutation, it becomes oncogenes that are dangerous for the existing cell. The stimulation of the uncontrolled cell division is because of deficiency of tumor suppressor genes. Therefore, in the past three decades, studies on a substantial volume of information about genes and proteins with their relationship to cancer growth had been investigated [6–8]. Recently, the role of mutated genes in cancer cells is very important. Hence, the potency of gene expression and defective proteins becomes the important discoveries to detect the novel cancer biomarkers [9].

The cancer cell has the ability to invade the local tissue and move to the other part of the body. This process is known as metastasis which is famously known as the key event to cancer cell invasion. The metastasis process is the major contributor to the high mortality cases among cancer patients. Normally, the invasion of cancer occurs when the tumor has reached a certain size and the peripheral rim of the cells has started to separate. In order to allow the tumor to grow further, the cancer cells innovate several methods of invasion both individually or in combination.

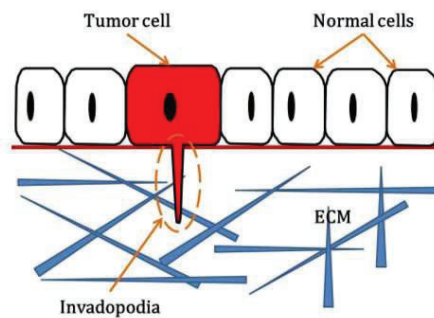


Figure 1.1: The invadopodium formation on the plasma membrane of the tumor cell [10].

In invasive cancer cells, specialized sub-cellular membrane structures that carry out a pivotal process in cancer cell invasion termed invadopodia are observed. Invadopodia are small punctuated finger-like protrusions that can be spotted on the membrane of cancer cells. Many kinds of proteins are recruited to invadopodia and these structures are responsible for high levels of proteolysis during cancer cell invasion and metastasis. Mentioned by [11], the invadopodia is the actin-based protrusions of the tumor cells. These specialized sub-cellular membrane structures can be found on the plasma membrane of an invasive cancer cell (see Figure 1.1).

The signal transduction through the binding of ligand and receptor leads to the polymerization of actin. The actin polymerization consequently pushed the membrane of the migrating cells and enables the metastatic cancer cells to pass through it. As mentioned by [12], in invasive cancer cells, invadopodia are the invasive feet that carry out a pivotal role in the cancer cell invasion. In addition, [13], stated that invadopodia are the structure that initiates the cancer cell invasion through the metastasis process.

From the perspective of biology, the formation of invadopodia involved the molecular interaction of ligand, membrane-associated receptor, signal transduction, matrix metalloproteinases (MMPs), extracellular matrix (ECM), and actin. The tumor cells secreted matrix-degrading enzymes mainly of the type of MMPs and urokinase plasminogen for the process of degradation. Thus, the degradation of the matrix enabled the cancer cells to migrate and invade the secondary sites of the body. The consequence of the degradation of the ECM, the creation of ligand on the extracellular region will be imminent. Followed by the binding of the ligand with the membrane-associated receptor such as epidermal growth factor receptor stimulate the signal transduction. Hence, the stimulation of signal transduction initiates the polymerization of actin, and up-regulation of the MMPs.

A study on the invadopodia should be seen as an important stage in the area of cancer research because these structures are the beginning of the metastasis process and can directly contribute to the number of deaths among cancer patients [14]. In addition, a study on the invadopodia formation should be the crucial strategies to control and more seriously to stop the metastasis process [15].

1.2.2 Mathematical Point of View

From the mathematical point of view, the formation of invadopodia has been widely explored in terms of mathematical modeling. There are two types of approaches that have been considered which are the fixed and free boundary plasma membrane. The fixed boundary plasma membrane has been considered in [12]. The formation and maturation of invadopodia include the actin reorganization, ECM degradation, signaling process through the receptor, and MMPs delivery to the invasion front has been focused on through the explanation of four key variables such as actin, ligand, MMPs, and ECM. In addition, the effect of the MMPs rate constant has been marked to investigate the level of invasiveness of a cancer cell. The deficiency of this study is the region of actin becomes disconnected and actin is spotted in the extracellular region

where it contradicts the biological fact, that the actin must lie within the cancer cell, especially at the location of the invasion front. Besides, its polymerization activities exert some pushing forces for the movement of the cancer cell.

To overcome the insufficiency in the [12]'s model, [10] proposed the new variable which is signal transduction which lies inside the cell. This variable is not considered in [12]. Hence, the semi-complete model for the formation of invadopodia has been proposed. However, the one-dimensional signal transduction is taken in the mathematical modeling with the others variables are omitted for simplicity purposes. In the numerical part, the plasma membrane is treated as a free boundary to separate the activities on the intracellular and extracellular regions. Through this study, the movement of the plasma membrane is increased as time increases and in this state, the invadopodium should be formed.

The continuation study from [10] is conducted by [16] with considering a two-dimensional study of signal transduction. Hence, the formation of invadopodium as stated in [10] has been proven through this study. Apart from this, the density of signal transduction is observed to be higher in the area of the invadopodium formation.

In the meantime, [17] investigated the two-dimensional free boundary problem with the implementation of ligand and signal transduction to study the cell protrusions formation on the plasma membrane. Apart from this, the activities of actin polymerization that are taken from the gradient of the intracellular signal drive the motion of the interface. In the mathematical modeling part, the Laplace equation of signal transduction with Dirichlet condition inside the cell is coupled to the Laplace equation of ligand with the Neumann condition for the exterior region has been emphasized. This study also described the availability of regular and neighboring points consequent of boundary movement.

Currently, different approaches to mathematical modeling should be conducted as a technique to observe the formation of invadopodia. The mathematical modeling

for ligand and signal transduction by considering the Dirichlet boundary conditions in both regions also needs to be explored. In addition, the actin polymerization is the direct cause of the protrusions, and their activities moved the plasma membrane in the outward direction. Here, actin polymerization is accounted for as the velocity of the interface and is one of the crucial points in mathematical modeling.

Hence, two velocities have been selected which are without jump velocity as proposed by [10] and with jump velocity that is yet to be considered. The main purpose of applying the jump velocity is because of the possible interactions in the regions intracellular and extracellular. Meanwhile, ligand and signal transduction that are considered in the mathematical modeling also are in two different regions. Therefore, this study aims to make such an attempt.

1.3 Problem Statements

Cancer is one of the leading causes of mortality in the world. Each year the number of cancer patients increases and is attacking all categories of ages. Due to this serious issue, the study on cancer cell invasion is very crucial. One of the key processes that contribute to cancer cell invasion is the metastasis process. The metastasis process starts from the migration of tumor cells from their primary location and invades another tissue or organ. For this purpose, the metastatic cancer cells need to penetrate several physical barriers to escape from the primary tumor before spread to the other part of the body. In order to pass through these barriers, the finger-like actin-rich protrusions or invadopodia are formed and play their role. The research on the invadopodia formation mainly on the mathematical interpretation needs to be solved since it can be one of the useful efforts in mathematical biology and cancer studies.

The interest in studying the formation of invadopodia from the perspectives of mathematics has increased substantially over the past decades. A series study from

Chaplain *et al* (refer [18–22]) have investigated the formation of invadopodia through the mathematical modeling approach. Their study focused on the cancer cell invasion at the tissue level. However, within years, the cancer cell invasion at the sub-cellular level has become a great concern from researchers. Meanwhile, the invadopodia are confirmed to be one of the structures that can initiate the cancer cell invasion at the sub-cellular level. Hence, in recent years, the research on invadopodia has been a focus of study.

Some researchers have successfully shown the presence of the protrusions on the plasma membrane by considering the fixed plasma membrane, [12]. In addition, there are researchers that have described the movement of the plasma membrane as the free boundary, [10, 16, 17]. It is well known that the formation of invadopodia includes several molecular processes of ligand, signal transduction, membrane-associated receptor, ECM, MMPs, and actin. Currently, there are several mathematical models available to observe the formation of invadopodia.

Although extensive research works have been devoted, the two-dimensional ligand and signal transduction with Dirichlet boundary conditions has yet been considered. Moreover, a different approach for the velocity of the plasma membrane can be improved. The previous studies have described the movement of the free boundary plasma membrane with the implementation of the gradient of the inner signal. Nevertheless, jump velocity that is accounted as the difference of gradient between intracellular signal and extracellular ligand is interesting to be implemented due to two regions that have been considered which are intracellular and extracellular. Therefore, the interaction in both regions inevitably occurs.

Based on the aforementioned matters, this study is carried out to study the formation of invadopodia on the plasma membrane using two-dimensional quasi-static and unsteady ligand and signal transduction. There are two different velocities selected to solve for the velocity of the plasma membrane. Hence, this study explores the following research questions:

1. What is the simplified mathematical formulation of the invadopodia formation in [10] that considering only ligand and signal transduction variables?
2. How to solve the quasi-static and unsteady models numerically?
3. How does the interface, ligand, and signal profiles are important for the formation of invadopodia on the plasma membrane?

1.4 Objectives of the Study

This study investigates the two-dimensional mathematical model for the formation of invadopodia in an invasive cancer cell with the approaches of without and with jump velocities. Specifically, the objectives of this study are:

1. To formulate the simplified mathematical model of the invadopodia formation from [10], consisting only ligand and signal variables.
2. To develop numerical algorithms for the level set method using finite difference techniques in solving quasi-static and unsteady problems from the mathematical model in (i).
3. To analyze the graphical results of the interface, ligand, and signal profiles with the formation of protrusions on the plasma membrane.

1.5 Scope of the Study

This study is focused on the mathematical modeling that correlated to the formation of invadopodia on the plasma membrane of an invasive cancer cell. Two-dimensional mathematical modeling is investigated to gain a clearer view of the formation of invadopodia. Furthermore, both quasi-static and unsteady mathematical models for the ligand and signal transduction are considered in order to understand the mechanism of invadopodia formation. Two different approaches for the velocity of the

plasma membrane have been considered in this study to observe the behavior of the protrusions.

The proposed mathematical models are solved numerically by using the level set method and finite difference technique of second-order centered finite difference, and ghost fluid with linear extrapolation, as proposed by [17]. The level set function is employed to detect the movement of the plasma membrane while, the regular and neighboring points are discretized by using the second-order centered finite difference and ghost fluid with linear extrapolation, respectively. For the time derivative, the forward difference is performed. The following problems are discussed in Chapters 4 to 5 of this thesis:

1. the effect of without jump velocity and with jump velocity in the quasi-static ligand and signal transduction mathematical model for the formation of invadopodia, and
2. the effect of without jump velocity and with jump velocity in the unsteady ligand and signal transduction mathematical model for the formation of invadopodia.

Further, the numerical algorithms and discretization are developed and solved using MATLAB software to obtain the graphical results. The research framework in Figure 1.2 is a pictorial description for every step taken in this study.

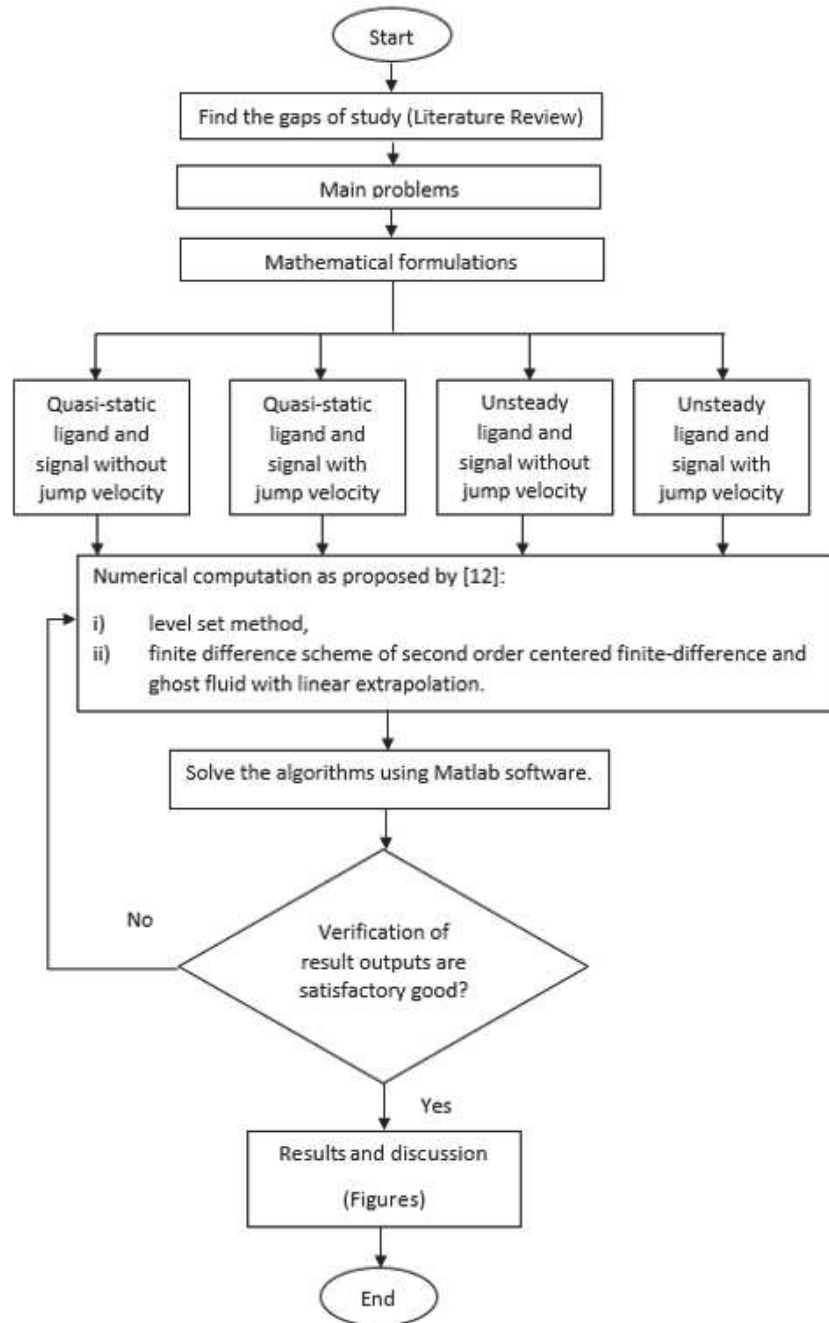


Figure 1.2: Research framework.

1.6 Significance of the Study

Most cancer patients do not aware that the cancer cells have been successfully spread to the secondary part of the body. This situation needs to be concerned as the secondary tumor is reported to be more dangerous when compared to the first tumor. Before the tumor cells are able to migrate from the primary location and invade another tissue or organ, the invasive cancer cells have to penetrate physical barriers to escape from the primary tumor. Here, the main role of the invadopodia takes place and degrades the extracellular matrix. Hence, the results from this study are significant and could be beneficial to mathematicians, biologists, and medical practices, according to the following reasons.

1. To build a better understanding of the biological process in the formation of invadopodia.
2. To become one of the efforts to cease the metastasis process.
3. The proposed variables such as ligand and signal transduction are indispensable for the formation of invadopodia. Hence, the results obtained from this study can be a new reference for medical experts to develop new therapies to control the invasiveness of cancer cells.
4. From the mathematical point of view, the employment of the free boundary plasma membrane can show a better insight into the movement of the plasma membrane.
5. Regarding the proposed method, the level set is the most suitable method since it can track the position of the free boundary over time. Meanwhile, it can distinguish the regions of the extracellular, and intracellular to separate the activities that happened at both regions.
6. The new approach of the velocity of the plasma membrane could provide the good reference needed in dealing with actin polymerization.

1.7 Thesis Organization

This thesis consists of six chapters, focusing on the problem of invadopodia formation on the plasma membrane by using two mathematical models (quasi-static and unsteady) with two approaches of velocity (without and with jump velocities). In Chapter 1, the background of the study is given, followed by the problem statements, objectives of the study, the scope of the study, and the significance of the study. The following Chapter 2 discusses some published research related to the proposed problems. In Chapter 3, the mathematical formulations involving the invadopodia formation in conjunction with the numerical discretizations are discussed in detail.

Chapter 4 presents the first problem of this study which is the quasi-static model of ligand and signal for the invadopodia formation. In this chapter, two approaches of velocity (without jump velocity and with jump velocity) to represent the velocity of the plasma membrane are included in the model.

Next, Chapter 5 is an extension of work in Chapter 4 which is by considering the unsteady model. Similar to the case in Chapter 4, the actin polymerization that is assumed as the velocity of the plasma membrane is accounted as the without jump velocity and with jump velocity.

In each chapter, the numerical results are discussed via graphical simulations of interface position, ligand, and signal densities. Finally, Chapter 6 summarizes and concludes the obtained results. The suggestions and recommendations for future research are also given in this last chapter. Meanwhile, all the references used are listed at the end of the thesis.

REFERENCES

1. Helfinger, V. and Schrder, K. Redox control in cancer development and progression. *Molecular Aspects of Medicine*. 2018. 63: 88 – 98. Signaling by Reactive Oxygen Species.
2. Organisation, W. H. Cancer. 2018. URL <https://www.who.int/cancer/en/>. accessed = 2019-09-19.
3. Noor, M. *Kanser wanita*. Utusan Publications. 2008. ISBN 9789676120656. URL <https://books.google.com.my/books?id=T0anpJSyuc0C>.
4. Malaysia, I. K. Cancer. URL <https://nci.moh.gov.my/index.php/ms/info/pencapaian-dan-statistik/>. accessed = 2022-07-04.
5. Lim, G. C. C. Overview of Cancer in Malaysia. *Japanese Journal of Clinical Oncology*. 2002. 32(supplement 1): S37–S42.
6. Francesca, Z., Michelangelo, C. and Stefano, P. YAP/TAZ at the roots of cancer. *Cancer cell*. 2016. 29(6): 783–803.
7. Gerard, B. L., Daria, V. G. and Scott, A. A. Exploiting the epigenome to control cancer-promoting gene-expression programs. *Cancer cell*. 2016. 29(4): 464–476.
8. Shufen, L., Jingming, L., Chen, C., Rongsheng, Z. and Kankan, W. Pan-cancer analysis of long non-coding RNA NEAT1 in various cancers. *Genes & diseases*. 2018. 5(1): 27–35.
9. Hassanpour, S. H. and Dehghani, M. Review of cancer from perspective of molecular. *Journal of Cancer Research and Practice*. 2017. 4(4): 127 – 129.
10. Admon, M. A. *Mathematical Modeling and Simulation in an Individual Cancer Cell Associated with Invadopodia Formation*. Osaka University, Japan: Ph.D. Thesis. 2015.

11. Stylli, S. S., Kaye, A. H. and Lock, P. Invadopodia: At the cutting edge of tumour invasion. *Journal of Clinical Neuroscience*. 2008. 15(7): 725 – 737.
12. Saitou, T., Rouzaimaimaiti, M., Koshikawa, N., Seiki, M., Ichikawa, K. and Suzuki, T. Mathematical modeling of invadopodia formation. *Journal of Theoretical Biology*. 2012. 298: 138 – 146.
13. Meirson, T. and Gil-Henn, H. Targeting invadopodia for blocking breast cancer metastasis. *Drug Resistance Updates*. 2018. 39: 1 – 17.
14. Seyfried, T. N. and Huysentruyt, L. C. On the origin of cancer metastasis. *Critical Reviews in Oncogenesis*. 2013. 18(1-2).
15. Paz, H., Pathak, N. and Yang, J. Invading one step at a time: the role of invadopodia in tumor metastasis. *Oncogene*. 2014. 33(33): 4193–4202.
16. Noor Azhuan, N., Poignard, C., Suzuki, T., Shafie, S. and Admon, M. Two-Dimensional Signal Transduction during the Formation of Invadopodia. *Malaysian Journal of Mathematical Sciences*. 2019. 13(2): 155–164.
17. Gallinato, O., Ohta, M., Poignard, C. and Suzuki, T. Free boundary problem for cell protrusion formations: theoretical and numerical aspects. *Journal of Mathematical Biology*. 2017. 75(2): 263–307.
18. Chaplain, M. and Lolas, G. Mathematical modelling of cancer invasion of tissue: Dynamic heterogeneity. *Networks and Heterogeneous Media*. 2006. 1.
19. Ramis-Conde, I., Chaplain, M. A. and Anderson, A. R. Mathematical modelling of cancer cell invasion of tissue. *Mathematical and Computer Modelling*. 2008. 47(5): 533 – 545. Towards a Mathematical Description of Cancer: Analytical, Numerical and Modelling Aspects.
20. Gerisch, A. and Chaplain, M. A. Mathematical modelling of cancer cell invasion of tissue: local and non-local models and the effect of adhesion. *Journal of Theoretical Biology*. 2008. 250(4): 684–704.
21. SZYMAŃSKA, Z., Rodrigo, C. M., LACHOWICZ, M. and Chaplain, M. A. Mathematical modelling of cancer invasion of tissue: the role and effect of

- nonlocal interactions. *Mathematical Models and Methods in Applied Sciences*. 2009. 19(02): 257–281.
22. Andasari, V., Gerisch, A., Lolas, G., South, A. and Chaplain, M. Mathematical modeling of cancer cell invasion of tissue: Biological insight from mathematical analysis and computational simulation. *Journal of mathematical biology*. 2011. 63: 141–71.
 23. Powathil, G., Gordon, K., Hill, L. and Chaplain, M. Modelling the effects of cell-cycle heterogeneity on the response of a solid tumour to chemotherapy: biological insights from a hybrid multiscale cellular automaton model. *Journal of theoretical biology*. 2012. 308: 1–19.
 24. Powathil, G., Swat, M. and Chaplain, M. Systems Oncology: Towards patient-specific treatment regimes informed by multiscale mathematical modelling. *Seminars in cancer biology*. 2014. 30. doi:10.1016/j.semcancer.2014.02.003.
 25. Powathil, G., Munro, A., Chaplain, M. and Swat, M. Bystander effects and their implications for clinical radiation therapy: Insights from multiscale in silico experiments. *Journal of Theoretical Biology*. 2014. 401. doi: 10.1016/j.jtbi.2016.04.010.
 26. Wang Z., D. T. S. Mathematical modeling in cancer drug discovery. *Drug Discov Today*. 2014. 19(2): 145–50.
 27. Halbrook, C. and Lyssiotis, C. Employing Metabolism to Improve the Diagnosis and Treatment of Pancreatic Cancer. *Cancer cell*. 2017. 31 1: 5–19.
 28. Tolde, O., Rsel, D., Vesel, P., Folk, P. and Brbek, J. The structure of invadopodia in a complex 3D environment. *European Journal of Cell Biology*. 2010. 89(9): 674 – 680.
 29. Cooper, G. M. and Hausman, R. E. *The Cell: A Molecular Approach, 4th Ed.* Sinauer Associates Incorporated. 2007.
 30. Li B., D. C. X. J. D. W., Gordon G. M. Specific killing of Rb mutant cancer cells by inactivating TSC2. *Cancer Cell*. 2010. 17(5): 469–80.

31. Szabó, A. and Merks, R. M. H. Cellular Potts Modeling of Tumor Growth, Tumor Invasion, and Tumor Evolution. In *Front. Oncol.* 2013.
32. Suzuki, T., Minerva, D., Nishiyama, K., Koshikawa, N. and Chaplain, M. A. J. Study on the tumor-induced angiogenesis using mathematical models. *Cancer Science.* 2018. 109(1): 15–23.
33. Kubo, A. and Suzuki, T. Mathematical models of tumour angiogenesis. *Journal of Computational and Applied Mathematics.* 2007. 204(1): 48 – 55. Special issue dedicated to Professor Shinnosuke Oharu on the occasion of his 65th birthday.
34. Billy, F., Ribba, B., Saut, O., Morre-Trouilhet, H., Colin, T., Bresch, D., Boissel, J.-P., Grenier, E. and Flandrois, J.-P. A pharmacologically based multiscale mathematical model of angiogenesis and its use in investigating the efficacy of a new cancer treatment strategy. *Journal of Theoretical Biology.* 2009. 260(4): 545 – 562.
35. Cai, Y., Xu, S., Wu, J. and Long, Q. Coupled modelling of tumour angiogenesis, tumour growth and blood perfusion. *Journal of Theoretical Biology.* 2011. 279(1): 90 – 101.
36. Olsen, M. M. and Siegelmann, H. T. Multiscale Agent-based Model of Tumor Angiogenesis. *Procedia Computer Science.* 2013. 18: 1016 – 1025. 2013 International Conference on Computational Science.
37. Santagiuliana, R., Ferrari, M. and Schrefler, B. Simulation of angiogenesis in a multiphase tumor growth model. *Computer Methods in Applied Mechanics and Engineering.* 2016. 304: 197 – 216.
38. Yamaguchi, H. Pathological roles of invadopodia in cancer invasion and metastasis. *European journal of cell biology.* 2012. 91: 902–7.
39. Meyers, R. A. *Cancer: From Mechanisms to Therapeutic Approaches.* WILEY-VCH Verlag GmbH & Co. KGaA, Weinheim. 2007.
40. Franssen, L. T. B. A. E. F. C. M. A., L. C. A Mathematical Framework for Modelling the Metastatic Spread of Cancer. *Bull Math Biol.* 2019. 81: 19652010.

41. Beraud, G. Mathematical models and vaccination strategies. *Vaccine*. 2018. 36(36): 5366 – 5372. Progress in Vaccines.
42. Li, D., Mu, C. and Yi, H. Global boundedness in a three-dimensional chemotaxis-haptotaxis model. *Computers & Mathematics with Applications*. 2019. 77(9): 2447 – 2462.
43. Kolbe, N., Kat'uchova, J., Sfakianakis, N., Hellmann, N. and Lukacova-Medvid'ova, M. A study on time discretization and adaptive mesh refinement methods for the simulation of cancer invasion: The urokinase model. *Applied Mathematics and Computation*. 2016. 273: 353 – 376.
44. Sulman, M. and Nguyen, T. A positivity preserving adaptive moving mesh method for cancer cell invasion models. *Journal of Computational and Applied Mathematics*. 2019. 361: 487 – 501.
45. Ganesan, S. and Lingeshwaran, S. Galerkin finite element method for cancer invasion mathematical model. *Computers & Mathematics with Applications*. 2017. 73(12): 2603 – 2617.
46. Ganesan, S. and Lingeshwaran, S. A biophysical model of tumor invasion. *Communications in Nonlinear Science and Numerical Simulation*. 2017. 46: 135 – 152.
47. Jiang, W., Sanders, A., Katoh, M., Ungefroren, H., Gieseler, F., Prince, M., Thompson, S., Zollo, M., Spano, D., Dhawan, P., Sliva, D., Subbarayan, P., Sarkar, M., Honoki, K., Fujii, H., Georgakilas, A., Amedei, A., Niccolai, E., Amin, A., Ashraf, S., Ye, L., Helferich, W., Yang, X., Boosani, C., Guha, G., Ciriolo, M., Aquilano, K., Chen, S., Azmi, A., Keith, W., Bilsland, A., Bhakta, D., Halicka, D., Nowsheen, S., Pantano, F. and Santini, D. Tissue invasion and metastasis: Molecular, biological and clinical perspectives. *Seminars in Cancer Biology*. 2015. 35: S244 – S275. A broad-spectrum integrative design for cancer prevention and therapy.

48. Nguyen Edalgo, A., Y.T.; Ford Versypt. Mathematical Modeling of Metastatic Cancer Migration through a Remodeling Extracellular Matrix. *Processes*. 2018. 6: 58.
49. Simmons, A., Burrage, P., Nicolau, D. V., Lakhani, S. and Burrage, K. Environmental factors in breast cancer invasion: a mathematical modelling review. *Pathology*. 2017. 49. doi:10.1016/j.pathol.2016.11.004.
50. Jiang, Y., Pjesivac-Grbovic, J., Cantrell, C. and Freyer, J. P. A multiscale model for avascular tumor growth. *Biophysical journal*. 2005. 89: 38843894.
51. Osborne, J., Walter, A., Kershaw, S., Mirams, G., Fletcher, A., Pathmanathan, P., Gavaghan, D., Jensen, O., Maini, P. and Byrne, H. A hybrid approach to multi-scale modelling of cancer. *Philosophical transactions. Series A, Mathematical, physical, and engineering sciences*. 2010. 368: 5013–28.
52. Rahman, M. M., Feng, Y., Yankeelov, T. E. and Oden, J. T. A fully coupled spacetime multiscale modeling framework for predicting tumor growth. *Computer Methods in Applied Mechanics and Engineering*. 2017. 320: 261 – 286.
53. Gallinato, O., Colin, T., Saut, O. and Poignard, C. Tumor growth model of ductal carcinoma: from in situ phase to stroma invasion. *Journal of Theoretical Biology*. 2017. 429: 253 – 266.
54. Cameron, L., Soneral, P., Soo, F. and Theriot, J. Secrets of actin-based motility revealed by a bacterial pathogen. *Nature reviews. Molecular cell biology*. 2000. 1: 110–9. doi:10.1038/35040061.
55. Augoff, K., Hryniewicz-Jankowska, A. and Tabola, R. Invadopodia: clearing the way for cancer cell invasion. *Annals of Translational Medicine*. 2020. 8: 902–902. doi:10.21037/atm.2020.02.157.
56. Beaty, B. T. and Condeelis, J. Digging a little deeper: The stages of invadopodium formation and maturation. *European Journal of Cell Biology*. 2014. 93(10): 438 – 444. Cell Migration and Invasion in Physiology and Pathology.

57. Parekh, A., Ruppender, N., Branch, K., Sewell-Loftin, M. K., Lin, J., Boyer, P., Candiello, J., Merryman, W. D., Guelcher, S. and Weaver, A. Sensing and Modulation of Invadopodia across a Wide Range of Rigidities. *Biophysical journal*. 2011. 100: 573–82.
58. Sibony-Benyamini, H. and Gil-Henn, H. Invadopodia: the leading force. *European journal of cell biology*. 2012. 91 11-12: 896–901.
59. Parekh, A. and Weaver, A. M. Regulation of invadopodia by mechanical signaling. *Experimental Cell Research*. 2016. 343(1): 89 – 95.
60. Jacob, A. and Prekeris, R. The regulation of MMP targeting to invadopodia during cancer metastasis. *Frontiers in Cell and Developmental Biology*. 2015. 3: 4.
61. Poincloux, R., Lizárraga, F. and Chavrier, P. Matrix invasion by tumour cells: a focus on MT1-MMP trafficking to invadopodia. *Journal of Cell Science*. 2009. 122(17): 3015–3024.
62. Hoshino, D., Koshikawa, N., Suzuki, T., Quaranta, V., Weaver, A. M., Seiki, M. and Ichikawa, K. Establishment and Validation of Computational Model for MT1-MMP Dependent ECM Degradation and Intervention Strategies. *PLOS Computational Biology*. 2012. 8(4): 1–10.
63. Jaboska-Trypu, A., Matejczyk, M. and Rosochacki, S. Matrix metalloproteinases (MMPs), the main extracellular matrix (ECM) enzymes in collagen degradation, as a target for anticancer drugs. *Journal of enzyme inhibition and medicinal chemistry*. 2016. 23: 1–7.
64. Hastie, E. L. and Sherwood, D. R. A new front in cell invasion: The invadopodial membrane. *European Journal of Cell Biology*. 2016. 95(11): 441 – 448. Integrated mechano-chemical signals in invasion.
65. Enderling, H., Alexander, N., Clark, E., Branch, K., Estrada, L., Crooke, C., Jourquin, J., Lobdell, N., Zaman, M., Guelcher, S., Anderson, A. and Weaver,

- A. Dependence of Invadopodia Function on Collagen Fiber Spacing and Cross-Linking: Computational Modeling and Experimental Evidence. *Biophysical journal*. 2008. 95: 2203–18.
66. Eckert, M. A., Lwin, T. M., Chang, A. T., Kim, J., Danis, E. and Ohno-Machado, . Y. J., L. Twist1-induced invadopodia formation promotes tumor metastasis. *Cancer cell*. 2011. 19: 372386.
67. Eddy, R., Weidmann, M., Sharma, V. and Condeelis, J. Tumor Cell Invadopodia: Invasive Protrusions that Orchestrate Metastasis. *Trends in Cell Biology*. 2017. 27.
68. Admon, M. A. and Suzuki, T. Signal transduction in the invadopodia formation using fixed domain method. *Journal of Physics: Conference Series*. 2017. 890: 012036.
69. Harskamp, G. R. v. G. H. e. a., L. The epidermal growth factor receptor pathway in chronic kidney diseases. *Nat Rev Nephrol*. 2016. 12: 496–506.
70. Christoph Wagener, O. M., Carol Stocking. *Cancer Signaling: From Molecular Biology to Targeted Therapy*. John Wiley & Sons. 2016.
71. Singh, I., Singh, G., Verma, V., Singh, S. and Chandra, R. In Silico Evaluation of Variable pH on the Binding of Epidermal Growth Factor Receptor Ectodomain to its Ligand Through Molecular Dynamics Simulation in Tumors. *Interdisciplinary Sciences: Computational Life Sciences*. 2019. 11(3): 437–443.
72. Bouchnita, A., Hellander, S. and Hellander, A. A 3D Multiscale Model to Explore the Role of EGFR Overexpression in Tumourigenesis. *Bulletin of mathematical biology*. 2019: 1–22.
73. Zhou, Y., Lee, J.-Y., Lee, C.-M., Cho, W.-K., Kang, M.-J., Koff, J. L., Yoon, P.-O., Chae, J., Park, H.-O., Elias, J. A. *et al*. Amphiregulin, an epidermal growth factor receptor ligand, plays an essential role in the pathogenesis of transforming growth factor- β -induced pulmonary fibrosis. *Journal of Biological Chemistry*. 2012. 287(50): 41991–42000.

74. Higashiyama, S., Iwabuki, H., Morimoto, C., Hieda, M., Inoue, H. and Matsushita, N. Membrane-anchored growth factors, the epidermal growth factor family: Beyond receptor ligands. *Cancer science*. 2008. 99(2): 214–220.
75. Kim, H. and Muller, W. J. The role of the epidermal growth factor receptor family in mammary tumorigenesis and metastasis. *Experimental cell research*. 1999. 253(1): 78–87.
76. Haiech, J., Gendraut, Y., Kilhoffer, M.-C., Ranjeva, R., Madec, M. and Lallement, C. A general framework improving teaching ligand binding to a macromolecule. *Biochimica et Biophysica Acta (BBA)-Molecular Cell Research*. 2014. 1843(10): 2348–2355.
77. Li, A., Dawson, J. C., Forero-Vargas, M., Spence, H. J., Yu, X., König, I., Anderson, K. and Machesky, L. M. The actin-bundling protein fascin stabilizes actin in invadopodia and potentiates protrusive invasion. *Current biology*. 2010. 20(4): 339–345.
78. Tehrani, S., Tomasevic, N., Weed, S., Sakowicz, R. and Cooper, J. A. Src phosphorylation of cortactin enhances actin assembly. *Proceedings of the National Academy of Sciences*. 2007. 104(29): 11933–11938.
79. Oser, M., Mader, C. C., Gil-Henn, H., Magalhaes, M., Bravo-Cordero, J. J., Koleske, A. J. and Condeelis, J. Specific tyrosine phosphorylation sites on cortactin regulate Nck1-dependent actin polymerization in invadopodia. *J Cell Sci*. 2010. 123(21): 3662–3673.
80. Mader, C. C., Oser, M., Magalhaes, M. A., Bravo-Cordero, J. J., Condeelis, J., Koleske, A. J. and Gil-Henn, H. An EGFR–Src–Arg–cortactin pathway mediates functional maturation of invadopodia and breast cancer cell invasion. *Cancer research*. 2011. 71(5): 1730–1741.
81. Ren, X., Qiao, Y., Li, J., Li, X., Zhang, D., Zhang, X., Zhu, X., Zhou, W., Shi, J., Wang, W. *et al.* Cortactin recruits FMNL2 to promote actin polymerization and endosome motility in invadopodia formation. *Cancer letters*. 2018. 419: 245–256.

82. Strychalski, W., Adalsteinsson, D. and Elston, T. Simulating Biochemical Signaling Networks in Complex Moving Geometries. *SIAM Journal on Scientific Computing*. 2010. 32(5): 3039–3070.
83. Shaikh, J., Bhardwaj, R. and Sharma, A. A Ghost Fluid Method Based Sharp Interface Level Set Method for Evaporating Droplet. *Procedia IUTAM*. 2015. 15: 124 – 131. IUTAM Symposium on Multiphase Flows with Phase Change: Challenges and Opportunities.
84. Osher, S. and Sethian, J. A. Fronts propagating with curvature-dependent speed: algorithms based on Hamilton-Jacobi formulations. *Journal of computational physics*. 1988. 79(1): 12–49.
85. Sethian, J. A. Theory, algorithms, and applications of level set methods for propagating interfaces. *Acta numerica*. 1996. 5(1): 309–395.
86. Chen, S., Merriman, B., Osher, S. and Smereka, P. A simple level set method for solving Stefan problems. *Journal of Computational Physics*. 1997. 135(1): 8–29.
87. Tan, L. and Zabaras, N. A level set simulation of dendritic solidification with combined features of front-tracking and fixed-domain methods. *Journal of Computational Physics*. 2006. 211(1): 36–63.
88. Tan, L. and Zabaras, N. A level set simulation of dendritic solidification of multi-component alloys. *Journal of Computational Physics*. 2007. 221(1): 9–40.
89. Tan, L. and Zabaras, N. Modeling the growth and interaction of multiple dendrites in solidification using a level set method. *Journal of Computational Physics*. 2007. 226(1): 131–155.
90. Wilder, J. W., Clemons, C., Golovaty, D., Kreider, K. L., Young, G. W. and Lillard, R. S. An adaptive level set approach for modeling damage due to galvanic corrosion. *Journal of Engineering Mathematics*. 2015. 91(1): 121–142.
91. Bajger, P., Ashbourn, J., Manhas, V., Guyot, Y., Lietaert, K. and Geris, L. Mathematical modelling of the degradation behaviour of biodegradable metals. *Biomechanics and modeling in mechanobiology*. 2017. 16(1): 227–238.

92. Coco, A. and Russo, G. Second order multigrid methods for elliptic problems with discontinuous coefficients on an arbitrary interface, I: one dimensional problems. *arXiv preprint arXiv:1111.1167*. 2011.
93. Coco, A. and Russo, G. Finite-difference ghost-point multigrid methods on Cartesian grids for elliptic problems in arbitrary domains. *Journal of Computational Physics*. 2013. 241: 464–501.
94. Coco, A., Currenti, G., Del Negro, C. and Russo, G. A second order finite-difference ghost-point method for elasticity problems on unbounded domains with applications to volcanology. *Communications in Computational Physics*. 2014. 16(4): 983–1009.
95. Coco, A. and Russo, G. Second order finite-difference ghost-point multigrid methods for elliptic problems with discontinuous coefficients on an arbitrary interface. *Journal of Computational Physics*. 2018. 361: 299 – 330.
96. Guyot, Y., Papantoniou, I., Chai, Y. C., Van Bael, S., Schrooten, J. and Geris, L. A computational model for cell/ECM growth on 3D surfaces using the level set method: a bone tissue engineering case study. *Biomechanics and modeling in mechanobiology*. 2014. 13(6): 1361–1371.
97. Gallinato, O. and Pognard, C. Superconvergent second order Cartesian method for solving free boundary problem for invadopodia formation. *Journal of Computational Physics*. 2017. 339: 412 – 431.
98. Leong, H., Robertson, A., Stoletov, K., Leith, S., Chin, C., Chien, A., Hague, M., Ablack, A., Carmine-Simmen, K., McPherson, V., Postenka, C., Turley, E., Courtneidge, S., Chambers, A. and Lewis, J. Invadopodia Are Required for Cancer Cell Extravasation and Are a Therapeutic Target for Metastasis. *Cell Reports*. 2014. 8(5): 1558 – 1570.
99. Sharma, V., Eddy, R., Entenberg, D., Kai, M., Gertler, F. and Condeelis, J. Tks5 and SHIP2 Regulate Invadopodium Maturation, but Not Initiation, in Breast Carcinoma Cells. *Current biology : CB*. 2013. 23: 2079–2089.

100. Chopp, D. L. Another Look At Velocity Extensions In The Level Set Method. *SIAM Journal on Scientific Computing*. 2009. 31(5): 3255–3273.
101. Adalsteinsson, D. and Sethian, J. The Fast Construction of Extension Velocities in Level Set Methods. *Journal of Computational Physics*. 1999. 148(1): 2–22.
102. Peng, D., Merriman, B., Osher, S., Zhao, H. and Kang, M. A PDE-Based Fast Local Level Set Method. *Journal of Computational Physics*. 1999. 155(2): 410–438.
103. Drummond, M. L., Li, M., Tarapore, E., Nguyen, T. T., Barouni, B. J., Cruz, S., Tan, K. C., Oro, A. E. and Atwood, S. X. Actin polymerization controls cilia-mediated signaling. *Journal of Cell Biology*. 2018. 217(9): 3255–3266.
104. Linder, S. and Kopp, P. Pedosomes at a glance. *Journal of Cell Science*. 2005. 118(10): 2079–2082.
105. Pourfarhangi, K. E., Bergman, A. and Gligorijevic, B. ECM Cross-Linking Regulates Invadopodia Dynamics. *Biophysical Journal*. 2018. 114(6): 1455–1466.
106. Saykali, B. A. and El-Sibai, M. Invadopodia, Regulation, and Assembly in Cancer Cell Invasion. *Cell Communication & Adhesion*. 2014. 21(4): 207–212.
107. Linder, S. and Kopp, P. Invadosomes at a glance. *Journal of Cell Science*. 2009. 122(17): 3009–3013.
108. Minna Takkunen, M. L. R. G. I. V., Mika Hukkanen. Podosome-like structures of non-invasive carcinoma cells are replaced in epithelial-mesenchymal transition by actin comet-embedded invadopodia. *Journal of Cellular and Molecular Medicine*. 2010. 14(6b): 1569–1593.
109. Revach, O.-Y. and Geiger, B. The interplay between the proteolytic, invasive, and adhesive domains of invadopodia and their roles in cancer invasion. *Cell Adhesion & Migration*. 2014. 8(3): 215–225.

110. Masi, I., Caprara, V., Bagnato, A. and Rosanò, L. Tumor cellular and microenvironmental cues controlling invadopodia formation. *Frontiers in Cell and Developmental Biology*. 2020: 1036.
111. Mogilner, A. and Oster, G. Cell motility driven by actin polymerization. *Biophysical journal*. 1996. 71(6): 3030–3045.
112. Pollard, T. D. and Cooper, J. A. Actin, a central player in cell shape and movement. *science*. 2009. 326(5957): 1208–1212.
113. Weaver, A. M. Invadopodia: specialized cell structures for cancer invasion. *Clinical & experimental metastasis*. 2006. 23(2): 97–105.
114. Kuo, T.-L., Cheng, K.-H., Shan, Y.-S., Chen, L.-T. and Hung, W.-C. β -catenin-activated autocrine PDGF/Src signaling is a therapeutic target in pancreatic cancer. *Theranostics*. 2019. 9(2): 324.

LIST OF PUBLICATIONS AND CONFERENCES

C.1 Indexed Journal

1. **Yaacob, N.,** Azhuan, N. A. N., Shafie, S., and Admon, M. A. (2019). Numerical Computation of Signal Stimulation from Ligand-EGFR Binding During Invadopodia Formation. *Matematika*, 35. (Indexed in Web of Science)
2. **Yaacob, N.,** Shafie, S., Suzuki, T., and Admon, M. A. (2021, July). Level set method for free boundary of invasive cancer cell using different functions of matrix metalloproteinases. In *Journal of Physics: Conference Series* (Vol. 1988, No. 1, p. 012020). IOP Publishing. (Indexed in Scopus)
3. **Yaacob, N.,** Shafie, S., Suzuki, T., and Admon, M. A. (2021, November). Mathematical modeling of quasi-static signal and ligand during invadopodia formation with velocity jump. In *AIP Conference Proceedings* (Vol. 2423, No. 1, p. 020037). AIP Publishing LLC. (Indexed in Scopus)
4. **Yaacob, N.,** Shafie, S., Suzuki, T., and Admon, M. A. (2022). Numerical computation of ligand and signal associated to invadopodia formation. *Jurnal Teknologi*, 84(4), 41-47. (Indexed in Web of Science)
5. **Yaacob, N.,** Shafie, S., Suzuki, T., and Admon, M. A. (2022). Signal transduction from ligand-receptor binding associated with the formation of invadopodia in an invasive cancer cell. *AIMS Bioengineering*, 9(3), 252-265. (Indexed in Web of Science)

C.2 Conference Proceedings

1. **Yaacob, N.,** Shafie, S., & Admon, M. A. (2020). Time-dependent signal transduction from ligand-epidermal growth factor receptor binding during invadopodia formation. Conference proceedings [eISSN: 2735-055X] of 8th International Graduate Conference on Engineering, Science and Humanities 2020 (IGCESH2020), Universiti Teknologi Malaysia.

C.3 Oral Presentations

1. **Yaacob, N.,** Azhuan, N. A. N., Shafie, S., & Admon, M. A. Numerical Computation of Signal Stimulation from Ligand-EGFR Binding During Invadopodia Formation. *7th International Conference and Workshop on Basic and Applied Sciences 2019 (ICOWOBAS 2019)*. July 16 - 17, 2019.
2. **Yaacob, N.,** Shafie, S., & Admon, M. A. Time-dependent signal transduction from ligand-epidermal growth factor receptor binding during invadopodia formation. *8th International Graduate Conference on Engineering, Science and Humanities 2020 (IGCESH2020)*. August 18 - 19, 2020.
3. **Yaacob, N.,** Shafie, S., Suzuki, T., & Admon, M. A. Mathematical Modeling of Quasi-Static Signal and Ligand during Invadopodia Formation with Velocity Jump. *International Conference on Mathematical Sciences and Technology 2020 (MATHTECH 2020)*. December 8 - 10, 2020.
4. **Yaacob, N.,** Shafie, S., Suzuki, T., & Admon, M. A. Level Set Method for Free Boundary of Invasive Cancer Cell using Different Functions of Matrix Metalloproteinases. *Symposium kebangsaan Sains Matematik ke-28 (SKSM 28)*. July 28 - 29, 2021.

C.4 Research Attachment

1. International Research Visit in Japan, Osaka University with Prof Clair Poinard and Prof Takashi Suzuki, 20-24 January 2020.

C.5 Award

1. **Best Paper** *Simposium Kebangsaan Sains Matematik ke-28 (SKSM 28)*
Yaacob, N., Shafie, S., Suzuki, T., & Admon, M. A. Level Set Method for Free Boundary of Invasive Cancer Cell using Different Functions of Matrix Metalloproteinases.